Environmental Modeling & Assessment (2023) 28:651–664
https://doi.org/10.1007/s10666-023-09876-3

Development of a New Event-Based Rainfall-Runoff Equation Based on Average Rainfall Intensity During an Event

Ali Shokri[1]

Received: 27 September 2022 / Accepted: 15 January 2023 / Published online: 24 January 2023

Abstract
Event-based rainfall-runoff models are practical tools commonly used to predict catchments' response to a rainfall event. However, one of the main concerns is that the characteristics of rain events are neglected in the model development. This paper develops a novel event-based rainfall-runoff equation to incorporate rainfall characteristics into account. The performance of the new equation is evaluated based on the root mean square error, Nash–Sutcliffe efficiency coefficient, and per cent bias for 13,339 rainfall-runoff events between 2005 and 2020 over 23 catchments across New Zealand and Australia with oceanic, mediterranean, tropical, subtropical, and semiarid climates. Compared to the previous event-based models, the new equation shows an improvement in runoff estimation in almost all case studies. Furthermore, considering the new equation is simple, efficient, and takes the rain event duration into account, the new equation has the potential to become a robust alternative method to the conventional curve number method in hydrological engineering projects.

Keywords Rainfall-runoff · Rain duration · Event-based · Runoff coefficient · Event average · Rainfall rate · IDF · Average rainfall rate

1 Introduction

The hydrological response of a catchment to a rainfall event is commonly known as a rainfall-runoff process [1]. A rainfall-runoff process often consists of complex physical procedures, i.e. interception, depression storage, evapotranspiration, infiltration, subsurface flow, groundwater flow, overland flow, and channel flow [2]. Previous studies indicate that rainfall characteristics such as rainfall rate, duration, and distribution, besides the catchment characteristics such as size, soil type, land use, and slope, can impact the occurrence and volume of runoff [3–6]. In addition, considering the physical condition of catchments is not homogenous, each catchment may respond differently to a rainfall event [1].

Several physically based mathematical expressions and computer simulation models have been developed that fully or partially represent the hydrological processes. Sometimes, infiltration equations are implemented to predict runoff from a rainfall event. The most common infiltration equations cited in the literature for rainfall-runoff modelling are Green-Ampt [7], Philip [8], Horton [8], Holtan [9], and Kostiakov [10] methods. In addition, sometimes, distributed surface water models are combined with distributed groundwater models to provide a better estimation [11–19]. However, these models are highly complex, data-hungry, and often require several spatial and temporal parameters, which in most cases are not readily available [20].

A simple alternative to physically based and continuous models is to estimate runoff from an individual rain event, often known as event-based models [21]. For example, the runoff coefficient has been used to estimate runoff from a rainfall event for many decades, which assumes that the depth of direct runoff is a percentage of the rainfall depth:

$$C = \frac{Q}{P}, \tag{1}$$

where C is the runoff coefficient, P is the total runoff depth, and Q is the total runoff depth in each rain event [22–25], or sometimes Q is the total direct runoff depth for each event [26–29], where "depth" refers to the total volume of runoff or direct runoff for each event over the catchment area. The terminology of "runoff coefficient" can be confusing as it

✉ Ali Shokri
ali.shokri@waikato.ac.nz

[1] School of Engineering, University of Waikato, Private Bag 3105, Hamilton 3240, New Zealand

is not consistent throughout the literature [30]. For example, the parameter called response factor [26], hydrologic response [27], runoff ratio [23], water yield [31], conversion efficiency [24], direct runoff response ratio [5], and runoff coefficient [6, 22, 28]. The other definition of runoff coefficients also can come from the rational method, which claims the peak flow is proportional to rainfall intensity for a given catchment [32]. For clarification, in the current study, the runoff coefficient means the total direct runoff over total precipitation for each rain event.

Even though the concept of estimating runoff for each event from runoff is attractive, the runoff coefficient is highly variable as the runoff coefficient is proportional to catchment and rainfall characteristics [3, 5].

The most popular event-based model by far is the soil conservation service (now the Natural Resources Conservation Service) curve number (SCS-CN) expression, which often is famous for its simplicity and applicability [33–35]. This method is widely used in practice and applied in many hydrologic applications. Some examples are flood prediction, water quality modelling, soil moisture balance, and sediment yields [36–46]. Also, several lumped and semi-distributed models are designed based on an adapted form of the SCS-CN equation, among which are CREAMS [47], GLEAMS [48], AGNPS [49], EPIC [50–52], WinTR-55 [53], HEC-HMS [54], EPA-SWMM [55], TOPNET [56], and SWAT [57].

The SCS-CN method originally comes from a lumped-based approach that calculates the total direct runoff from a storm event [58]. For deriving the SCS-CN expression, the proportionality between retention and runoff is assumed to be:

$$\frac{F}{S} = \frac{Q}{P}, \tag{2}$$

where F is the actual retention, S is the maximum potential retention, and Q is the total direct runoff during a rainfall event. Assuming:

$$F = P - Q, \tag{3}$$

and subtracting a certain amount of rainfall, referred to as initial abstraction from the total runoff depth P and solving Eq. 2 for Q yields:

$$Q = \frac{(P - I_a)^2}{P + S - I_a}, \text{when } P \geq Ia, \text{otherwise } Q = 0, \tag{4}$$

where I_a is the initial abstraction. Commonly, a linear correlation is assumed between S and I_a,

$$I_a = \lambda S, \tag{5}$$

where λ is the initial abstraction ratio. λ is considered 0.2 in the original formula [40, 59, 60]. However, the background of this assumption is known [58].

In the SI units,

$$S = \frac{25.4}{CN} - 0.254, \tag{6}$$

where CN value is defined by hydrological soil group, land use, hydrological surface condition, and soil moisture condition [41]. Theoretically, the CN may vary between 0 and 100.

From a hydrologic engineering perspective, the SCS-CN method is simple, transparent, appealing, and only requires one empirical parameter, the CN. The SCS is popular because SCS-CN databases can easily link to distributed soil and vegetation layers stored within a GIS [34]. Hawkins [41] reported that there is no alternative with the benefits of the curve number method available, and within its group, the SCS-CN method is monotypic. However, besides many advantages, too many ambiguities raise questions about this method's accuracy [33, 34, 41, 42]. For example, Eq. 2, as the central assumption of the SCS-CN method, has no physical justification [34].

Another concern is that the rainfall characteristics, such as rain duration, are neglected in the equation [61]. For example, the SCS-CN method does not count for the differences between 40 cm rainfall in 1 day and 10 days, while infiltration and runoff would be considerably different [32, 58]. However, several studies statistically indicated that the runoff is proportional to the rainfall duration [3–5].

This study aims to introduce a novel, robust, and simple equation for estimating runoff from a rain event by taking the rain event duration into consideration. The new equation only has one empirical parameter. However, compared to the other event-based models, it more precisely represents the physics of the rainfall-runoff process by incorporating rainfall characteristics.

2 Materials

2.1 Hydro-Meteorological Data

For this study, 23 catchments ranging from 0.3 to 564 km^2 are selected from catchments in New Zealand and Australia. The sites in New Zealand have an oceanic climate, with cool but not cold winters and warm summers. In contrast, the case studies in Australia have a range of climates, including Oceanic, Mediterranean, tropical, subtropical, and semi-arid climates. Commonly, no snow is recorded in any sites during the study periods.

Rain events are defined based on the minimum-interevent-time method [62], in which the beginning and end of each event are defined by a minimum rainless period of at least 24 h. The available data set is divided into the calibration and validation periods. In total, 13,339 events are observed across 23 study areas. In all cases, rainfalls are recorded either at the outlet or in the vicinity of the outlet. A summary of catchment size, climate type, calibration, and validation periods and the number of events are listed in Table 1.

2.1.1 Baseflow Separation

The quick flow (direct runoff), which is the direct response to a catchment to rainfall, is separated from the base flow, water seeping into the stream from groundwater. Therefore for the development of a rainfall-runoff model often, the quick flow is separated from the runoff. The BFI+, which is a powerful and user-friendly software with eleven methods for baseflow and quick flow separation methods, is selected [63, 64]. The *one-parameter recession digital filter* method in the BFI+software is used for baseflow quick-flow separation for the current study. As an example of baseflow separation, the base flow separation for the Opanuku river is shown in Fig. 1. Then, the direct runoff depth for each event is calculated by dividing the total direct runoff for each event over the catchment area.

3 Methods

3.1 Development of the New Equation

The event average rainfall rate is calculated for each event:

$$i_{av} = \frac{P}{t}, \tag{7}$$

where i_{av} is the average rainfall rate (mm/h) in each event, and t is the event duration (h). The existing correlation between runoff coefficient (Q/P) and average rainfall rate [1] has been suggested in previous studies. The correlation between the runoff coefficient and average rainfall rate in Opanuku and Pukekohe Ngakoroa rivers is illustrated in Fig. 2.

Considering the duration varies in each event, the proportionality between runoff and average rainfall rates (I_{av}) is not substantial.

Intensity–duration–frequency (IDF) curves were implemented to enhance the correlation by unifying rain event durations. The IDF curves concept was established in early 1930, and many mathematical expressions for IDF curves were suggested subsequently [32].

IDF curve can be expressed in a general form:

$$i_{av} = \frac{f(T)}{g(t)}, \tag{8}$$

where t is the rain storm duration, T is the storm event return period, $f(T)$ is a function of the return period, and $g(t)$ is a function of the storm duration t. $f(T)$ and $g(t)$ are unique functions for each site and can be estimated directly from previous rainfall records.

For this study, following a method suggested by [32, 65], the annual maximum rainfall for each site was rank-ordered, and the return period for each annual maximum rainfall value was estimated. Then, the rank-ordered rainfall value was divided by the event duration for each return period, resulting in the average intensity plotted versus the duration. As an example, the IDF curves of Pukekohe for return periods ranging from 0.01 to 100 years are given in Fig. 3.

For storms with a return period of T, Eq. 8 gives the following relation between the equivalent rainfall rate in 24 h and the rainfall rate in each rainstorm with a duration of t [32]:

$$f(T) = i_{av}g(t) = i_{24}g(24), \tag{9}$$

where i_{24} is the equivalent rainfall rate in 24 (h).

Rearranging for i_{24} yields:

$$i_{24} = \frac{g(t)}{g(24)} i_{av}. \tag{10}$$

Assuming a power function form for $g(t)$ after Koutsoyiannis et al. [66]:

$$g(t) = at^n, \tag{11}$$

where a and n are local constant variables obtained from the past rainfall records for each site.

Therefore,

$$g(24) = a(24)^n \tag{12}$$

Substituting $g(t)$ and $g(24)$ in Eq. 10 yields:

$$i_{24} = i_{av}\left(\frac{t}{24}\right)^n \tag{13}$$

Then, Eq. 13 is used to calculate i_{24} for all events. With the new adjustment on rainfall rate, the runoff coefficient shows a stronger correlation to i_{24} than i_{av} in all case studies.

For all sites, the n value is calculated using the IDF curves. For example, from the rainfall record of the Opanuku and Pukekohe Ngakoroa sites, the IDF curves are generated, and then the n value is calculated as 0.37 and 0.56, respectively. In the next step, i_{24} is calculated, and the relationships between the runoff coefficient and i_{24} are plotted in Fig. 4.

A comparison between Figs. 2 and 4 shows using i_{24} instead of i_{av} increases the R^2 by 47% (from R^2=0.38 to 0.56)

Table 1 A summary of catchment size, study period, and the number of events for each catchment in New Zealand (NZ) and Australia (AUS)

Site No.	Site name	Location	Area (km2)	Climate	Calibration		Validation	
					Period (years)	No. of events	Period (years)	No. of events
1	West Hoe Heights	Auckland, West Hoe Heights, NZ	0.3	Oceanic	2008–2015	349	2015–2017	119
2	Mangemangeroa	Auckland, East Tamaki Heights, NZ	4.4	Oceanic	2008–2015	357	2015–2017	121
3	Pukekohe Ngakoroa	Auckland, Pukekohe, NZ	4.5	Oceanic	2009–2015	283	2015–2019	236
4	Arkins Creek	Victoria, Wyelangta, AUS	4.5	Oceanic	2005–2015	475	2015–2019	186
5	Wainui Te Whara	Bay of Plenty, Whakatane, NZ	5.4	Oceanic	2008–2015	331	2015–2020	267
6	Waingaehe	Bay of Plenty, Rotorua, NZ	9.5	Oceanic	2008–2015	329	2015–2019	243
7	Orewa	Auckland, Millwater, NZ	9.6	Oceanic	2007–2015	439	2015–2020	263
8	Maungaparerua	Northland, Kerikeri, NZ	11.7	Oceanic	2008–2015	357	2015–2018	184
9	Whangarei Ngunguru	Northland, Whangarei, NZ	12.5	Oceanic	2009–2015	313	2015–2018	193
10	Rutherford Creek	New South Wales, Brown Mountain, AUS	14.4	Oceanic	2005–2015	515	2015–2019	235
11	Opanuku	Auckland, Henderson, NZ	15.7	Oceanic	2007–2015	364	2015–2017	72
12	Fisher Creek	Queensland, Innisfail, AUS	16.2	Semi-arid	2005–2015	367	2015–2019	146
13	Raumanga	Northland, Whangarei, NZ	16.3	Oceanic	2008–2015	359	2015–2017	120
14	Scott Creek	South Australia, Adelaide Hills, AUS	29.0	Mediterranean	2005–2015	385	2015–2018	170
15	Gellibrand	Victoria, Melborne, AUS	52.7	Oceanic	2005–2015	455	2015–2019	186
16	Elizabeth Valley	Northern Territory, Darwin, AUS	95.6	Tropical	2005–2015	315	2015–2019	138
17	Tinana Creek	Queensland, north of the Sunshine coast, AUS	101.8	Subtropical	2005–2015	367	2015–2019	148
18	Mannus Creek	New South Wales, Tumbarumba, AUS	194.3	Oceanic	2005–2015	420	2015–2019	186
19	Bass River	Victoria, Melborne, AUS	240.2	Oceanic	2005–2015	501	2015–2019	205
20	South Johnstone River	Queensland, Central Mill, AUS	397.7	Subtropical	2005–2015	455	2015–2019	187
21	Ashley Gorge	Christchurch, Canterbury, NZ	472.0	Oceanic	2005–2015	503	2015–2020	293
22	Wakefield	South Australia, Adelaide, AUS	500.9	Semi-arid	2005–2015	360	2015–2019	146
23	Queanbeyan River	New South Wales, Canberra, AUS	563.7	Oceanic	2005–2015	506	2015–2019	190
	Total					9,105		4,234

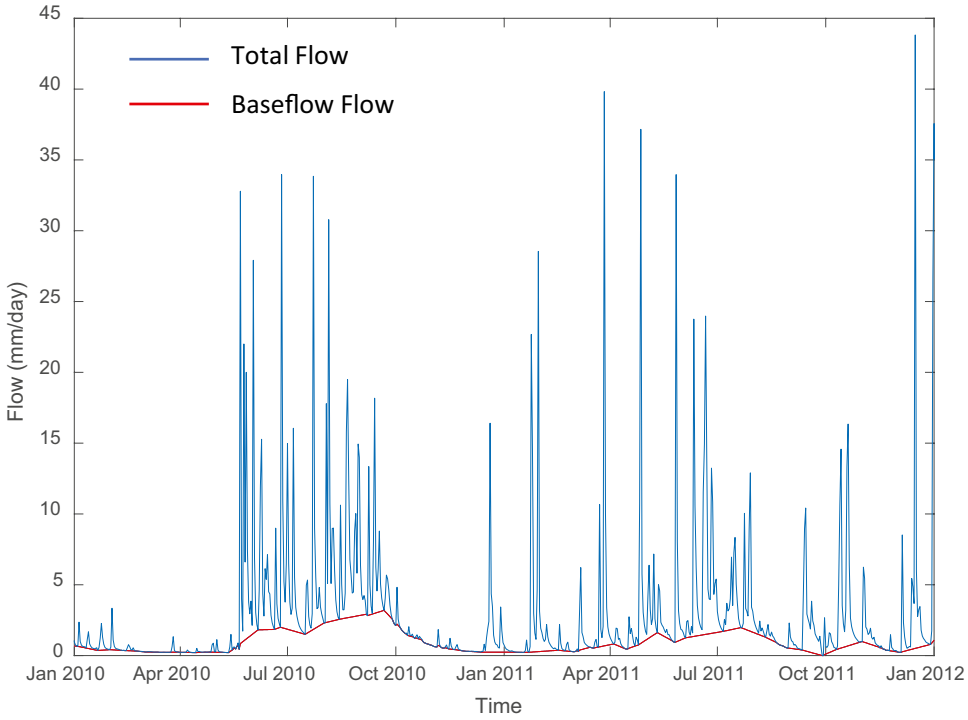

Fig. 1 An example of the base-flow separation for Opanuku using one parameter recession digital filter

in Opanuku and 104% (from $R^2=0.27$ to 0.55) in Pukekohe Ngakoroa sites. The same pattern is observed in the other case studies. A scatterplot and boxplot in Fig. 5 compare the correlation (R^2) of Q/P vs i_{av} and Q/P vs i_{24} for all case studies.

Considering all points in the scatterplot located above the 1:1 line indicates that using the IDF curves concept to unify the event durations effectively improved the runoff coefficient and rainfall rate significantly. A comparison between medians in the boxplot shows that the median of R^2 is increased by around 100% from $R^2=0.22$ in $Q_0/P-i_{av}$ to $R^2=0.44$ in $Q_0/P-i_{24}$.

Then, it is assumed that the runoff coefficient (Q/P) is directly proportional to i_{24}:

$$\frac{Q}{P} \propto i_{24} \tag{14}$$

Then, by multiplying the right side of the proportionality by a constant, α, the proportionality is replaced by an equation:

$$Q = \alpha i_{24} P, \tag{15}$$

where α (h/mm) is a local constant and varies for each site.

Substituting i_{24} from Eq. 13 in Eq. 15 yields:

$$Q = \alpha i_{av} \left(\frac{t}{24}\right)^n P, \tag{16}$$

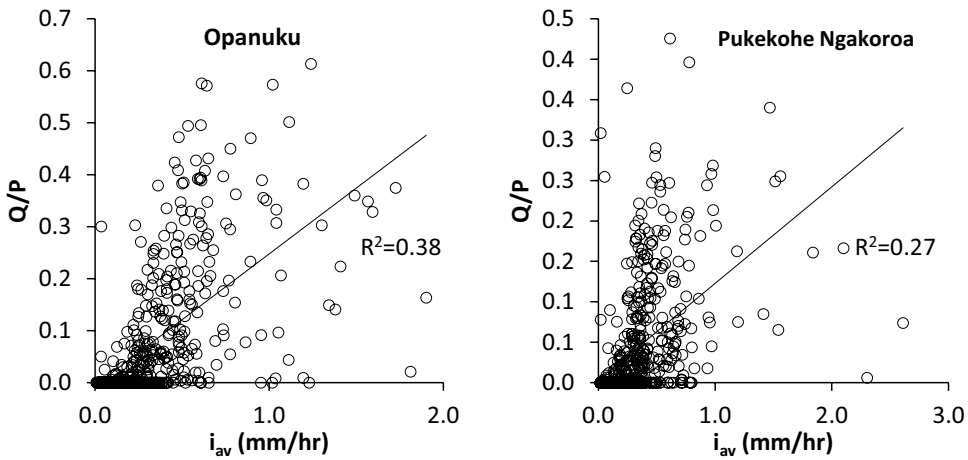

Fig. 2 Correlation between runoff coefficient (Q_0/P) and average rainfall rate in Opanuku and Pukekohe Ngakoroa rivers

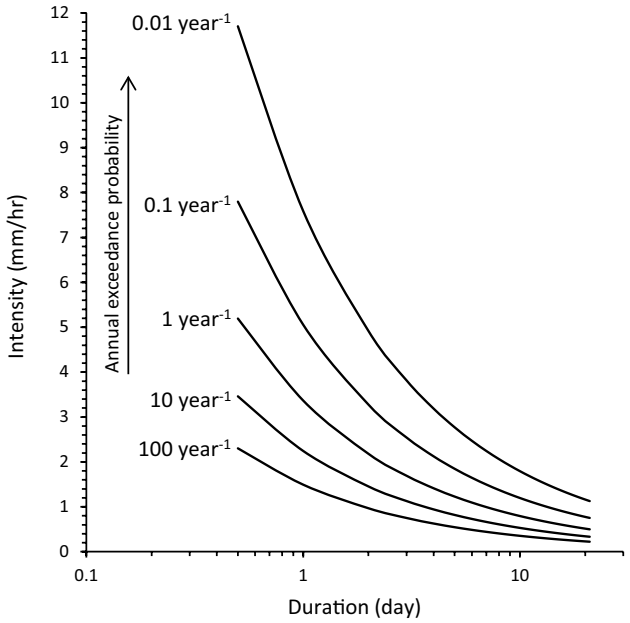

Fig. 3 IDF curves of Pukekohe for return periods ranging from 0.01 to 100 years

and substituting i_{av} from Eq. 7 in Eq. 16 yields:

$$Q = \frac{\alpha P^2}{t}\left(\frac{t}{24}\right)^n \tag{17}$$

From this point, Eq. 17 is known as the "new equation" in this paper. Considering quick flow data is used to develop the new equation, the concept of initial abstraction is already included in the P/Q correlation.

4 Results and Discussion

For all case studies, α and CN values were calculated using the least squares fitting technique to minimise the sum of the squared differences between the observed data and computed runoff from the new equation and SCS-CN methods.

$$\sum_{\text{Events}}\{Q_0 - Q_C\}^2 = \sum_{\text{Events}}\left\{Q_0 - \frac{\alpha P^2}{t}\left(\frac{t}{24}\right)^n\right\}^2 \overset{\text{by varying } \alpha}{\Rightarrow} \text{Minimum} \tag{18}$$

$$\sum_{\text{Events}}\{Q_0 - Q_C\}^2 = \sum_{\text{Events}}\left\{Q_0 - \frac{(P - I_a)^2}{P + S - I_a}\right\}^2 \overset{\text{by varying CN}}{\Rightarrow} \text{Minimum} \tag{19}$$

where Q_0 is the observed runoff depth, and Q_C is the calculated runoff depth from the new equation and SCS-CN method. The optimised CN and α values from the calibration process are listed in Table 2.

Also, as some examples, the observed and estimated runoff by the new equation and SCS-CN method versus the total rainfall for each event for Opanuku and Pukekohe Ngakoroasites are illustrated in Fig. 6.

The SCS-CN method predicts only a single value for each rainfall event regardless of the rainfall characterises. However, the new equation estimates various runoffs for each rainfall event depending on the rainfall durations. For example, looking at three extreme events around $P = 250$ mm in Pukekohe Ngakoroa (Fig. 5), the SCS-CN method predicts 71 mm for the three events. In contrast, the new equation predicts 42, 51, and 82 mm, respectively. Similarly, three different runoffs, 29, 36 and 83 mm, are also observed at the outlet.

As a way of comparison, the estimated runoff by the new equation and SCS-CN method is plotted against the observed runoff for the Opanuku river in Fig. 7.

The R^2 in the SCS-CN plot is around 23% lower than the R^2 in the new equation (from $R^2 = 0.79$ to 0.64). Also, the slope of the linear trendline in the new equation is closer to the 1:1 line than the SCS-CN. So, overall, the new equation shows a better performance in the runoff depth estimation than the SCS-CN method in the Opanuku river for the study period.

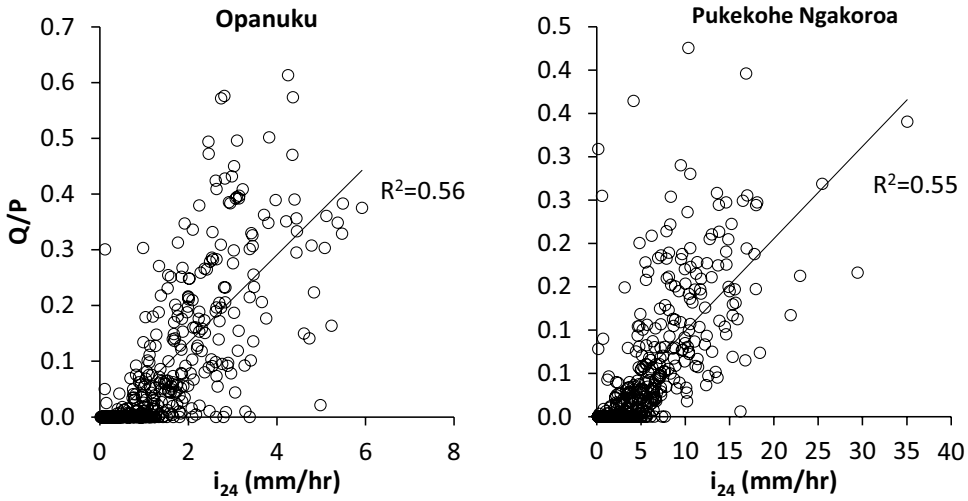

Fig. 4 Correlation between runoff coefficient (Q/P) and i_{24} in Opanuku and Pukekohe Ngakoroa sites

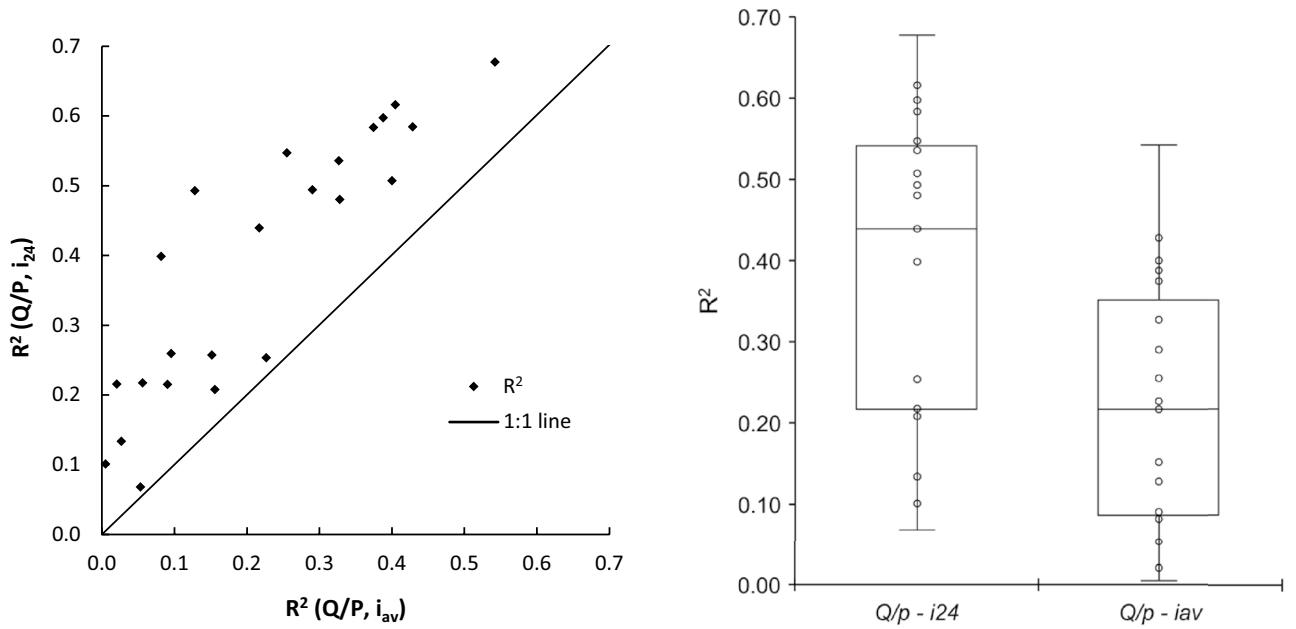

Fig. 5 Scatterplot and boxplot compare the correlation (R^2) of Q/F vs i_{24} and Q/P vs i_{av} for all case studies

4.1 The Performance Evaluation Strategies

Three statistical criteria were used to evaluate the new equation and SCS-CN performances.

4.1.1 Root Mean Square Error (RMSE)

$$\mathrm{RMSE} = \sqrt{\frac{1}{m}\sum_{\mathrm{Events}}\left(Q_O - Q_C\right)^2} \tag{20}$$

where m is the total number of events. $RMSE = 0$ indicates the perfect model fit, and the closer the $RMSE$ values are to zero, the better the model performance.

4.1.2 Nash–Sutcliffe Model Efficiency (NSE)

The Nash–Sutcliffe model efficiency coefficient [67] that is often used for evaluation of the performance of hydrologic models [68, 69] is calculated for both methods:

$$\mathrm{NSE} = 1 - \frac{\sum_{\mathrm{Events}}\left(Q_O - Q_C\right)^2}{\sum_{\mathrm{Events}}\left(Q_O - \overline{Q_O}\right)^2} \tag{21}$$

where $\overline{Q_O}$ is the mean of observed flow depth, and NSE is the Nash–Sutcliffe model efficiency coefficient. The NSE values range from $-\infty$ to 1, where 1 shows a perfect prediction, whereas $NSE \leq 0$ suggests that a simple average of observed values is better than the model estimations. Therefore, the model performance is unacceptable.

4.1.3 Percent Bias (PBIAS)

$PBIAS$ measures the average tendency of the predicted flow depth to be larger or smaller than the observed data [70].

$$\mathrm{PBIAS} = \left[\frac{\sum_{\mathrm{Events}}\left(Q_O - Q_C\right)}{\sum_{\mathrm{Events}}\left(Q_O\right)}\right] \times 100 \tag{22}$$

A low-magnitude value indicates an accurate model simulation where 0 is a perfect fit. Positive values suggest model underestimates, and negative values indicate model overestimates.

4.2 Calibration

$RMSE$, NSE, and $PBIAS$ were calculated for the calibration periods for all case studies. A summary of the calibrated values (CN and α) and performance evaluation of the new equation and SCS-CN models in the calibration process are listed in Table 2.

Overall, the new equation shows a better performance compared to the SCS-CN model. For example, the average NSE of the new equation for 23 case studies is 0.74, which is 25% higher than the NSE of the SCS-CN. Likewise, the average $RMSE$ improved to 14%. Scatterplots in Fig. 8 compare the NSE and $PBIAS$ of the new equation with the SCS-CN for each case study.

Table 2 A summary of the calibrated values, *CN* and α, and the new equation (NE) and SCS-CN models' performance in the calibration process based on *NSE*, *RMSE*, and *PBIAS* for all case studies

Site no.	Site name	Calibrated values		NSE		RMSE (mm)		PBIAS	
		CN	Alpha (h/mm)	SCS*	NE**	SCS	NE	SCS	NE
1	West Hoe Heights	77	0.2522	0.62	0.73	10.1	8.5	12%	2%
2	Mangemangeroa	61	0.0634	0.67	0.75	4.1	3.5	32%	5%
3	Pukekohe Ngakoroa	52	0.0574	0.46	0.74	3.8	2.6	48%	11%
4	Arkins Creek	36	0.0148	0.35	0.67	0.6	0.4	100%	−6%
5	Wainui Te Whara	66	0.0769	0.78	0.81	5.1	4.7	24%	11%
6	Waingaehe	23	0.0087	0.08	0.61	0.9	0.6	92%	18%
7	Orewa	67	0.1074	0.59	0.66	6.9	6.3	28%	16%
8	Maungaparerua	76	0.1092	0.81	0.79	10.3	10.6	5%	11%
9	Whangarei Ngunguru	68	0.1307	0.82	0.92	10.6	7.1	7%	0%
10	Rutherford Creek	55	0.0452	0.90	0.88	2.5	2.7	6%	−28%
11	Opanuku	62	0.2016	0.61	0.80	8.0	5.7	27%	−1%
12	Johnson River	30	0.0134	0.56	0.63	17.3	15.8	34%	14%
13	Fisher Creek	27	0.0831	0.62	0.73	25.7	21.9	33%	6%
14	Raumanga	59	0.0606	0.88	0.94	4.2	2.9	29%	10%
15	Scott Creek	49	0.0106	0.23	0.48	2.2	1.8	53%	6%
16	Gellibrand	36	0.0253	0.81	0.89	3.5	2.6	42%	−13%
17	Elizabeth Valley	33	0.0601	0.72	0.81	15.9	13.0	29%	−10%
18	Tinana Creek	48	0.0388	0.85	0.84	8.8	8.9	10%	−10%
19	Mannus Creek	59	0.0929	0.34	0.50	3.1	2.7	38%	−26%
20	Bass River	61	0.0536	0.49	0.53	3.8	3.6	25%	−14%
21	Ashley Gorge	68	0.0743	0.73	0.75	5.0	4.8	25%	3%
22	Wakefield	50	0.0001	0.23	0.60	0.7	0.5	47%	−79%
23	Queanbeyan	41	0.0005	0.91	0.92	1.0	0.9	29%	22%
	MAX	77	0.2522	0.91	0.94	25.70	21.88	100%	22%
	Average	52	0.0687	0.61	0.74	6.69	5.74	34%	−2%
	Median	55	0.0601	0.62	0.75	4.22	3.62	29%	3%
	Min	23	0.0001	0.08	0.48	0.60	0.44	5%	−79%
	SD	16	0.0715	0.24	0.14	7.18	6.21	27%	21%

SCS-CN method

NE, new equation

In the *NSE* scatterplot, points above 1:1 lines indicate the new equation performs better, whereas, in the *RMSE* scatterplot, points below the 1:1 line mean the new equation performs better on that specific site. In the *NSE* scatterplot, apart from 3 sites where the SCS-CN method performs slightly better, the new equation has supremacy over the SCS-CN model in predicting flow. Similarly, the *RMSE* indicator also shows that the new equation predominantly performs better in all case studies apart from one site. Figure 9 shows a scatterplot that compares the α and *CN* for 23 case studies.

The scatterplot shows a relatively weak to moderate correlation between α value and *CN* with an R^2 of 0.42. It means the higher the α value in a catchment, the less

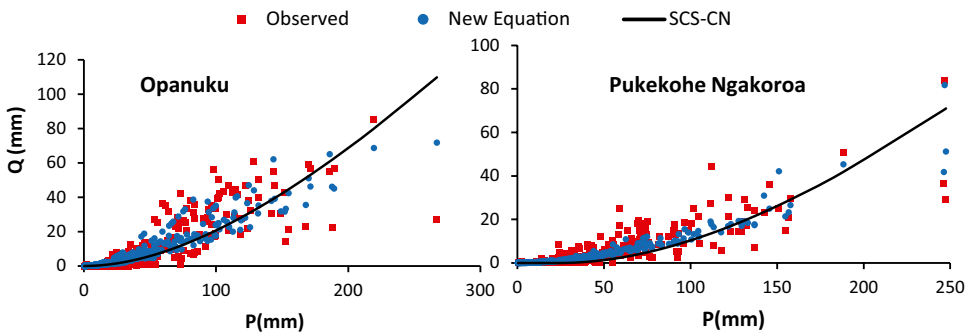

Fig. 6 Observed and calculated direct runoff estimation with the new equation and SCS-CN method in Opanuku and Pukekohe Ngakoroa rivers

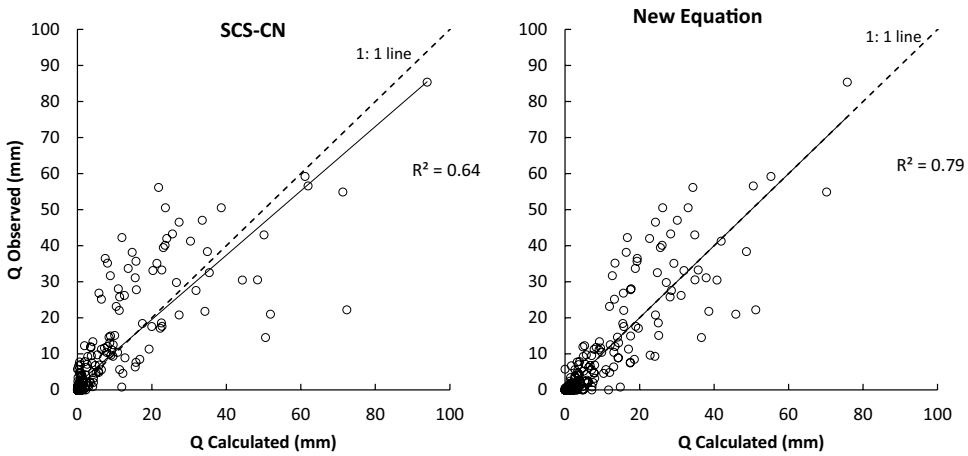

Fig. 7 Calculated runoff depth from the new equation and SCS-CN versus observed runoff depth in the Opanuku river

rainfall infiltrates the groundwater system and generates more runoff.

4.3 Validation

For validation, the calculated values for *CN* and α from the calibration process were directly used in the SCS-CN and the new equation on the validation data sets, defined in Table 1. A summary of *NSE*, *RMSE*, and *PBIAS* for the validation process is listed in Table 3.

A comparison between the calibration and validation performances shows that in both models, all performance indicators are slightly dropped in the calibration process. For example, the average *NSE* in the SCS-CN equation is lower by 26% (from 0.59 in calibration to 0.45), and *NSE* in the new equation declined by 21% (from 0.74 in calibration to 0.59).

However, similar to the calibration, in most case studies, the new equation performs better than the SCS-CN method in the validation process. For example, on average, *NSE* in the new equation for all case studies is 34% higher than SCS-CN performance. Likewise, the average *RMSE* in the new equation is higher by 9. However, there are a few cases where SCS-CN performs the same or marginally better than the new equation in the validation process.

There are some cases where both models perform exceptionally well, for example, in Rutherford Creek and Elizabeth Valley case studies. But there are some cases in which both models failed to predict runoff depth, for instance, Wakefield and West Hoe Heights.

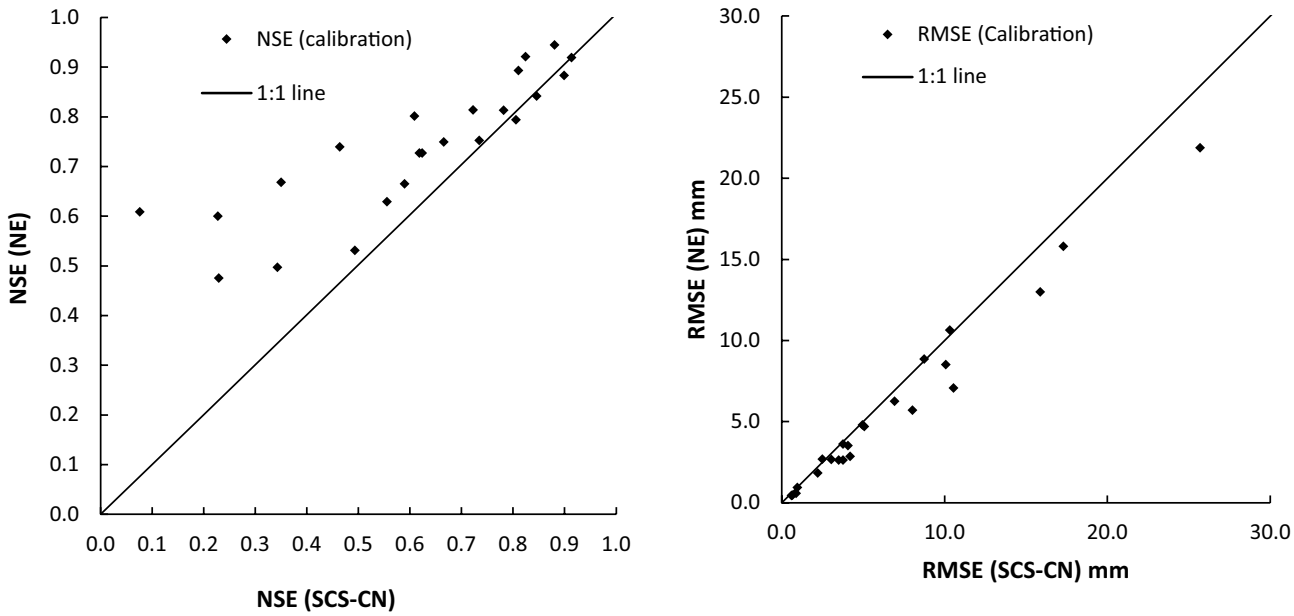

Fig. 8 A comparison between *NSE* and *RMSE* of the new equation (NE) and SCS-CN for the calibration process

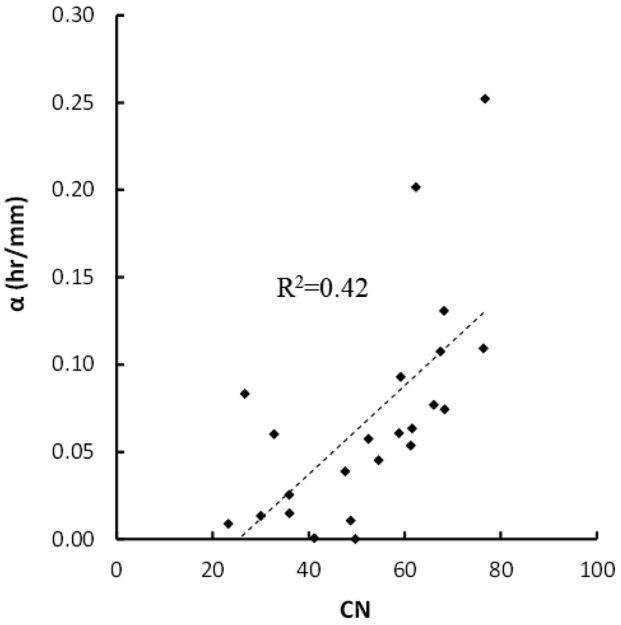

Fig. 9 A comparison between the α and *CN* for all case studies

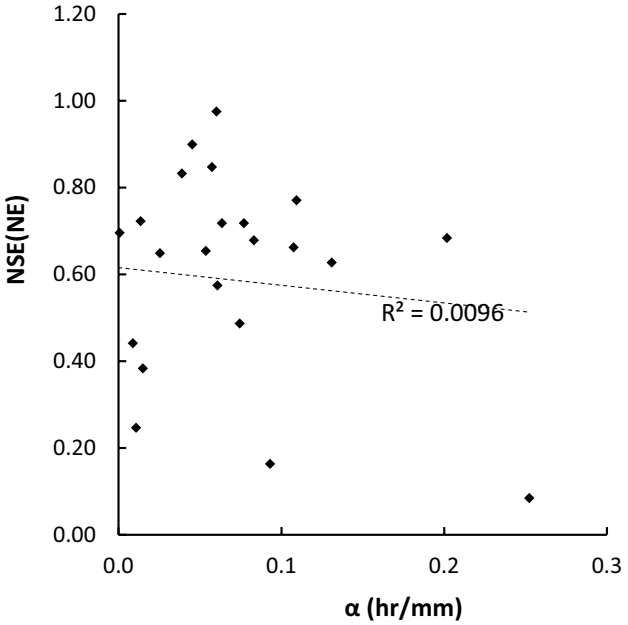

Fig. 10 A comparison between the new equation performance (NSE) and the α value

Table 3 A summary of the validation of the new equation (NE) and the SCS-CN model based on the performance evaluation techniques, including *NSE*, *RMSE*, and *PBIAS* for all sites

Site no.	Site name	NSE		RMSE (mm)		PBIAS	
		SCS*	NE**	SCS	NE	SCS	NE
1	West Hoe Heights	0.06	0.09	27.9	27.6	0%	−11%
2	Mangemangeroa	0.67	0.72	6.5	6.0	35%	19%
3	Pukekohe Ngakoroa	0.41	0.85	7.0	3.6	10%	6%
4	Arkins Creek	0.11	0.38	0.5	0.4	100%	−48%
5	Wainui Te Whara	0.58	0.72	4.9	4.0	8%	−8%
6	Waingaehe	0.02	0.44	1.2	0.9	94%	15%
7	Orewa	0.59	0.66	6.7	6.1	30%	14%
8	Maungaparerua	0.76	0.77	10.0	9.7	−1%	8%
9	Whangarei Ngunguru	0.70	0.63	11.5	12.8	3%	−3%
10	Rutherford Creek	0.92	0.90	3.4	3.8	32%	5%
11	Opanuku	−0.26	0.68	15.5	7.7	−13%	−29%
12	Johnson River	0.66	0.72	19.1	17.1	22%	8%
13	Fisher Creek	0.65	0.68	31.0	29.8	0%	−5%
14	Raumanga	0.29	0.57	4.6	3.5	31%	−4%
15	Scott Creek	0.16	0.25	5.1	4.8	86%	63%
16	Gellibrand	0.17	0.65	4.1	2.7	85%	7%
17	Elizabeth Valley	0.98	0.98	5.3	6.3	24%	−19%
18	Tinana Creek	0.81	0.83	3.5	3.3	−6%	−62%
19	Mannus Creek	0.00	0.16	2.7	2.5	45%	−33%
20	Bass River	0.73	0.65	1.8	2.0	18%	−49%
21	Ashley Gorge	0.44	0.49	6.0	5.8	10%	−14%
22	Wakefield	−0.01	−0.01	4.0	4.0	100%	77%
23	Quenbeyan	0.88	0.70	1.0	1.6	50%	55%
	MAX	0.98	0.98	31.0	29.8	100%	77%
	Average	0.45	0.59	8.0	7.2	33%	0%
	Median	0.58	0.66	5.1	4.0	24%	−3%
	Min	−0.26	−0.01	0.5	0.4	−13%	−62%
	SD	0.36	0.27	9.3	8.9	38%	37%

SCS-CN method

NE, new equation

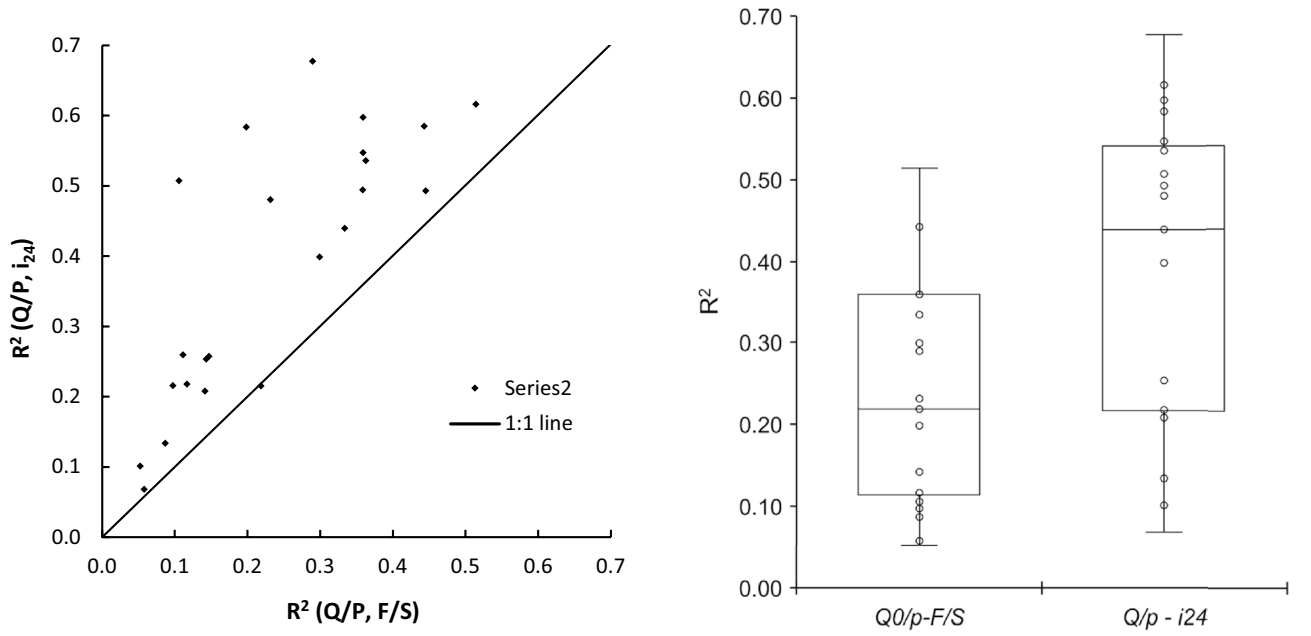

Fig. 11 Scatterplot and boxplot compare R^2 of Q/F -i_{24} and Q/P -F/S as the central assumption of the new equation and the SCS-CN methods, respectively

Figure 10 shows no correlation between the new equation performance (*NSE*) and the α value. Considering that the α value represents the capacity of catchments to generate runoff, the lack of a correlation means the performance of the new equation is independent of the α value and can be used in a wide range of catchments.

In general, it can be concluded that the new equation is a robust alternative to the conventional models in oceanic climate conditions. This research also studied a few catchments in Mediterranean, tropical, subtropical, and semi-arid classmates. However, no advantage or disadvantage is observed in the performance of the new equation in different climates. However, the numbers of samples in each climate are relatively small. Therefore, further investigation with a broader range of climates is required to conclude whether the new equation performs reasonably in all climate conditions.

4.4 Discussion on the Core Assumption of the New Equation and the SCS-CN Method

The proportionality of Q/S vs F/S (Eq. 2) and Q/S vs i_{24} (Eq. 14) are the central assumptions for SCS-CN and the new equation, respectively. In order to investigate the validity of these assumptions, the R^2 of Q_0/P vs F/S, and Q_0/P vs i_{24} for all case studies are calculated. Equations 3, 6, 8, and 13 are used to calculate F, S, i_{av}, and i_{24}, respectively. A scatterplot and a boxplot in Fig. 11 compare the R^2 of Q_0/P vs F/S and i_{24} for all case studies.

From the boxplot, the median R^2 of Q_0/P vs i_{24} is 0.44, which is 101% higher than the R^2 of Q_0/P vs F/S. Also, a one-to-one compression in the scatterplot shows that all points are above the 1:1 line in the advantage of the new equation. Therefore, it can be concluded that the central assumption of the new equation (Eq. 14) is more reliable than the central assumption of the SCS-CN method (Eq. 2).

5 Conclusion

A new empirical event-based rainfall-runoff equation was developed. The IDF curve concept was implemented to introduce a 24-h event average rainfall (i_{24}) for each rain event. An acceptable correlation between the runoff coefficient (Q/P) and i_{24} was observed. Based on this correlation, a new equation was developed. The new equation and SCS-CN equation were used to estimate runoff for 23 catchments across New Zealand and Australia with oceanic and semi-arid climates ranging from 0.3 to 584 km^2. Statistical indicators such as *NSE*, *RMSE*, and *PBIAS* were used to compare the predictive skill of the new equation and SCS-CN. It was shown that the new equations perform better in both calibration and validation processes. Therefore, it can be concluded that the new equation is a robust alternative to the conventional event-based model in oceanic and semi-arid climate conditions. Also, there is a possibility that the new equation will be valid in other climate conditions. However, it needs further investigation.

Author Contribution Not applicable.

Funding Open Access funding enabled and organized by CAUL and its Member Institutions.

Data Availability All data that support the findings of this study are available from public websites.

Declarations

Ethical Approval Not applicable.

Conflict of Interest The author declares no competing interests.

References

1. Critchley, W., Siegert, K., & Chapman, C. (1991). A manual for the design and construction of water harvesting schemes for plant production. *Food and Agriculture Organization of the United Nations - Rome*.
2. Kisi, O., Shiri, J., & Tombul, M. (2013). Modeling rainfall-runoff process using soft computing techniques. *Computers and Geosciences*. https://doi.org/10.1016/j.cageo.2012.07.001
3. Hewlett, J. D., Fortson, J. C., & Cunningham, G. B. (1977). The effect of rainfall intensity on storm flow and peak discharge from forest land. *Water Resources Research*. https://doi.org/10.1029/WR013i002p00259
4. Hewlett, J. D., & Bosch, J. M. (1984). The dependence of storm flows on rainfall intensity and vegetal cover in South Africa. *Journal of Hydrology*. https://doi.org/10.1016/0022-1694(84)90060-X
5. Howard, A. J., Bonel, M., Gilmour, D., & Cassells, D. (2010). Is rainfall intensity significant in the rainfall-runoff process within tropical rainforests of northeast Queensland? The Hewlett regression analyses revisited. *Hydrological Processes*. https://doi.org/10.1002/hyp.7694
6. Sarwar, M. W., Campbell, D. I., & Shokri, A. (2022). Riparian zone as a variable source area for the estimation of evapotranspiration through the analysis of daily fluctuations in streamflow. *Hydrological Processes*, *36*(10). https://doi.org/10.1002/hyp.14708
7. Green, W. H., & Ampt, G. (1911). Studies on soil physics: I. Flow of air and water throught soils. *Journal of Agricultural Science*.
8. Hillel, D. (2013). Introduction to soil physics. *Introduction to Soil Physics*. https://doi.org/10.1016/C2009-0-03052-9
9. Holtan, H. N., States., U., & Agriculture., D. of. (1961). A concept for infiltration estimates in watershed engineering. [Washington, D.C.]: United States Dept. of Agriculture. Retrieved from https://archive.org/details/conceptforinfilt51holt
10. Ghosh, R. K. (1985). A note on Lewis-Kostiakov's infiltration equation. *Soil Science*. https://doi.org/10.1097/00010694-198503000-00001
11. Kollet, S. J., and R. M. M. (2008). Capturing the influence of groundwater dynamics on land surface processes using an integrated, distributed watershed model. *Water Resources Research*, *44*(2). https://doi.org/10.1029/2007WR006004
12. Kollet, S. S. J., & Maxwell, R. R. M. (2006). Integrated surface – Groundwater flow modeling: A free-surface overland flow boundary condition in a parallel groundwater flow model. *Advances in Water Resources, 29*, 945–958. https://doi.org/10.1016/j.advwatres.2005.08.006
13. Maxwell, R., & Miller, N. L. (2005). Development of a coupled land surface and groundwater model. *Journal of Hydrometeorology, 6*(3), 233–247. https://doi.org/10.1175/JHM422.1
14. Shokri, A., & Bardsley, W. E. (2016). Development, testing and application of DrainFlow: A fully distributed integrated surface-subsurface flow model for drainage study. *Advances in Water Resources, 92*, 299–315. https://doi.org/10.1016/j.advwatres.2016.04.013
15. Shokri, A. (2011). Developing a new numerical surface/subsurface model for irrigation and drainage system design. In *IAHS-AISH Publication, 345*, 75–79.
16. Shen, C., & Phanikumar, M. S. (2010). A process-based, distributed hydrologic model based on a large-scale method for surface – Subsurface coupling. *Advances in Water Resources, 33*(12), 1524–1541. https://doi.org/10.1016/j.advwatres.2010.09.002
17. Camporese, M., Paniconi, C., Putti, M., & Orlandini, S. (2010). Surface-subsurface flow modeling with path-based runoff routing, boundary condition-based coupling, and assimilation of multisource observation data. *Water Resources Research, 46*(2), W02512. https://doi.org/10.1029/2008WR007536
18. Brunner, P., & Simmons, C. T. (2012). HydroGeoSphere: A fully integrated, physically based hydrological model. *Ground Water, 50*(2), 170–176. https://doi.org/10.1111/j.1745-6584.2011.00882.x
19. Kumar, M., Duffy, C. J., & Salvage, K. M. (2009). A second-order accurate, finite volume–based, integrated hydrologic modeling (FIHM) framework for simulation of surface and subsurface flow. *Vadose Zone Journal, 8*(4), 873. https://doi.org/10.2136/vzj2009.0014
20. Sivapalan, M. (2005). 13 pattern, process and function: Elements of a unified theory of hydrology at the catchment scale. *In Encyclopedia of Hydrological Sciences*. https://doi.org/10.1002/0470848944.hsa012
21. Stephens, C. M., Johnson, F. M., & Marshall, L. A. (2018). Implications of future climate change for event-based hydrologic models. *Advances in Water Resources*. https://doi.org/10.1016/j.advwatres.2018.07.004
22. Savenije, H. H. G. (1996). The runoff coefficient as the key to moisture recycling. *Journal of Hydrology*. https://doi.org/10.1016/0022-1694(95)02776-9
23. McNamara, J. P., Kane, D. L., & Hinzman, L. D. (1998). An analysis of streamflow hydrology in the Kuparuk River Basin, Arctic Alaska: A nested watershed approach. *Journal of Hydrology*. https://doi.org/10.1016/S0022-1694(98)00083-3
24. Burch, G. J., Bath, R. K., Moore, I. D., & O'Loughlin, E. M. (1987). Comparative hydrological behaviour of forested and cleared catchments in southeastern Australia. *Journal of Hydrology*. https://doi.org/10.1016/0022-1694(87)90171-5
25. Iroumé, A., Huber, A., & Schulz, K. (2005). Summer flows in experimental catchments with different forest covers, Chile. *Journal of Hydrology*. https://doi.org/10.1016/j.jhydrol.2004.06.014
26. Hewlett, J. D., & Hibbert, A. R. (1967). Factors affecting the response of small watersheds to precipitation in humid areas. *Forest hydrology*. https://doi.org/10.1177/0309133309338118

27. Woodruff, J. F., & Hewlett, J. D. (1970). Predicting and mapping the average hydrologic response for the Eastern United States. *Water Resources Research*. https://doi.org/10.1029/WR006i005p01312
28. van Dijk, A. I. J. M., Bruijnzeel, L. A., Vertessy, R. A., & Ruijter, J. (2005). Runoff and sediment generation on bench-terraced hillsides: Measurements and up-scaling of a field-based model. *Hydrological Processes*. https://doi.org/10.1002/hyp.5629
29. Schellekens, J., Scatena, F. N., Bruijnzeel, L. A., van Dijk, A. I. J. M., Groen, M. M. A., & van Hogezand, R. J. P. (2004). Stormflow generation in a small rainforest catchment in the Luquillo experimental forest, Puerto Rico. *Hydrological Processes*. https://doi.org/10.1002/hyp.1335
30. Blume, T., Zehe, E., & Bronstert, A. (2007). Rainfall-runoff response, event-based runoff coefficients and hydrograph separation. *Hydrological Sciences Journal*. https://doi.org/10.1623/hysj.52.5.843
31. Sidle, R. C., Tsuboyama, Y., Noguchi, S., Hosoda, I., Fujieda, M., & Shimizu, T. (2000). Stormflow generation in steep forested headwaters: A linked hydrogeomorphic paradigm. *Hydrological Processes*. https://doi.org/10.1002/(SICI)1099-1085(20000228)14:3%3c369::AID-HYP943%3e3.0.CO;2-P
32. Chin, D. A. (2000). *Water-resources engineering*. Prentice Hall.
33. Ponce, V. M., & Hawkins, R. H. (1996). Runoff curve number: Has it reached maturity? *Journal of Hydrologic Engineering, 1*(1), 11–19. https://doi.org/10.1061/(ASCE)1084-0699(1996)1:1(11)
34. Beven, K. J. (2012). Rainfall-runoff modelling: The primer. *Rainfall-Runoff Modelling: The Primer: Second Edition*. https://doi.org/10.1002/9781119951001
35. Soulis, K. X., Valiantzas, J. D., Dercas, N., & Londra, P. A. (2009). Investigation of the direct runoff generation mechanism for the analysis of the SCS-CN method applicability to a partial area experimental watershed. *Hydrology and Earth System Sciences*. https://doi.org/10.5194/hess-13-605-2009
36. Abon, C. C., David, C. P. C., & Pellejera, N. E. B. (2011). Reconstructing the tropical storm Ketsana flood event in Marikina River, Philippines. *Hydrology and Earth System Sciences*. https://doi.org/10.5194/hess-15-1283-2011
37. Steenhuis, T. S., Winchell, M., Rossing, J., Zollweg, J. A., & Walter, M. F. (2002). SCS runoff equation revisited for variable-source runoff areas. *Journal of Irrigation and Drainage Engineering*. https://doi.org/10.1061/(asce)0733-9437(1995)121:3(234)
38. Soulis, K. X., Ntoulas, N., Nektarios, P. A., & Kargas, G. (2017). Runoff reduction from extensive green roofs having different substrate depth and plant cover. *Ecological Engineering*. https://doi.org/10.1016/j.ecoleng.2017.01.031
39. Van Dijk, A. I. J. M. (2010). Selection of an appropriately simple storm runoff model. *Hydrology and Earth System Sciences*. https://doi.org/10.5194/hess-14-447-2010
40. Woodward, D. E., Hawkins, R., Jiang, R., Hjelmfelt A., J., Van Mullem, J., Quan, Q. D., & Dc, W. (2003). Runoff curve number method: Examination of the initial abstraction ratio. *In World Water & Environmental Resources Congress,* 1–10. https://doi.org/10.1061/40685(2003)308
41. Hawkins, R. H. (2014). Curve number method: Time to think anew? *Journal of Hydrologic Engineering*. https://doi.org/10.1061/(asce)he.1943-5584.0000954
42. Garen, D. C., & Moore, D. S. (2005). Curve number hydrology in water quality modeling: Uses, abuses, and future directions. *Journal of the American Water Resources Association*. https://doi.org/10.1111/j.1752-1688.2005.tb03742.x
43. Mishra, S. K., Tyagi, J. V., Singh, V. P., & Singh, R. (2006). SCS-CN-based modeling of sediment yield. *Journal of Hydrology*. https://doi.org/10.1016/j.jhydrol.2005.10.006
44. Singh, P. K., Bhunya, P. K., Mishra, S. K., & Chaube, U. C. (2008). A sediment graph model based on SCS-CN method. *Journal of Hydrology*. https://doi.org/10.1016/j.jhydrol.2007.11.004
45. Soulis, K. X. (2018). Estimation of SCS curve number variation following forest fires. *Hydrological Sciences Journal*. https://doi.org/10.1080/02626667.2018.1501482
46. Soulis, K. X., & Valiantzas, J. D. (2013). Identification of the SCS-CN parameter spatial distribution using rainfall-runoff data in heterogeneous watersheds. *Water Resources Management, 27*(6), 1737–1749. https://doi.org/10.1007/s11269-012-0082-5
47. Kinsei W.G. (1980). CREAMS: A field scale model for chemicals, runoff, and erosion from agricultural. *Management Systems*.
48. Knisel, W. G., Davis, F. M., & Specialist, C. (2000). Groundwater loading effects of agricultural management systems. *Area*.
49. Young, R. A., Onstad, C., Bosch, D., & Anderson, W. (1989). AGNPS: A nonpoint-source pollution model for evaluating agricultural watersheds. *Journal of Soil and Water Conservation*.
50. Williams, J. R., & Sharply, A. N. (1989). EPIC--Erosion/Productinity Impact Calculator: 1. Model documentation. *USDA Technical Bulletin No. 1768*, (1768 Pt 1).
51. Williams, J. R. and S. V. P. (1995). The EPIC model. *Computer models of watershed hydrology.*
52. Sharpley, a. N., & Williams, J. R. (1990). EPIC: The erosion-productivity impact calculator. *U.S. Department of Agriculture Technical Bulletin*.
53. Karl Visser, & Claudia Scheer. (2013). The new USDA-NRCS WinTR-55 small watershed hydrology model. https://doi.org/10.13031/2013.10431
54. Feldman, A. (2000). *Hydrologic modeling system HEC-HMS. Hydrologic Modeling System HEC-HMS Technical Reference Manual.*
55. Rossman, L. (2015). Storm water management model user's manual version 5.1. United States Environment Protection Agency. https://www.epa.gov/sites/default/files/2019-02/documents/epaswmm5_1_manual_master_8-2-15.pdf
56. Clark, M. P., Rupp, D. E., Woods, R. A., Zheng, X., Ibbit, R. P., Slater, A. G., Uddstrom, M. J. (2008). Hydrological data assimilation with the ensemble kalman filter: Use of streamflow observations to update states in a distributed hydrological model. *Advances in Water Resources, 31*(10), 1309–1324. https://doi.org/10.1016/j.advwatres.2008.06.005
57. Neitsch, S., Arnold, J., Kiniry, J., & Williams, J. (2009). Soil & water assessment tool theoretical documentation version. *Texas Water Resources Institute, TR-406*.
58. Hawkins, R., Ward, T., Woodward, D., and Van Mullem, J. (2008). Curve number hydrology: State of the practice. *Curve Number Hydrology.* https://doi.org/10.1061/9780784410042.ch01
59. Yuan, Y., Nie, W., Mccutcheon, S. C., & Taguas, E. V. (2014). Initial abstraction and curve numbers for semiarid watersheds in Southeastern Arizona. *Hydrological Processes*. https://doi.org/10.1002/hyp.9592
60. Shi, Z. H., Chen, L. D., Fang, N. F., Qin, D. F., & Cai, C. F. (2009). Research on the SCS-CN initial abstraction ratio using rainfall-runoff event analysis in the Three Gorges Area, China. *Catena*. https://doi.org/10.1016/j.catena.2008.11.006
61. Mishra, S. K., Singh, V. P., & S. P. K. (2018). Revisiting the soil conservation service curve number method. In H. Modeling (Ed.), *Water Science and Technology Library* (pp. 667–693). Springer.
62. Dunkerley, D. (2008). Identifying individual rain events from pluviograph records: A review with analysis of data from an Australian dryland site. *Hydrological Processes*. https://doi.org/10.1002/hyp.7122
63. Chapman, T., & Maxwell, A. (1996). Baseflow separation - comparison of numerical methods with tracer experiments. In *23rd Hydrology and Water Resources Symposium*.
64. Lyne, V. D., & Hollick, M. (1979). Stochastic time-variable rainfall-runoff modelling. In *In Institute of Engineers Australia National Conference*.

65. Sun, Y., Wendi, D., Kim, D. E., & Liong, S. Y. (2019). Deriving intensity–duration–frequency (IDF) curves using downscaled in situ rainfall assimilated with remote sensing data. *Geoscience Letters*. https://doi.org/10.1186/s40562-019-0147-x
66. Koutsoyiannis, D., Kozonis, D., & Manetas, A. (1998). A mathematical framework for studying rainfall intensity-duration-frequency relationships. *Journal of Hydrology*. https://doi.org/10.1016/S0022-1694(98)00097-3
67. Nash, J. E., Sutcliffe, & V., I. (1970). River flow forecasting through conceptual models, part 1 - A discussion of principles. *Journal of Hydrology*, *10*.
68. Deshmukh, D. S., Chaube, U. C., Ekube Hailu, A., Aberra Gudeta, D., & Tegene Kassa, M. (2013). Estimation and comparision of curve numbers based on dynamic land use land cover change, observed rainfall-runoff data and land slope. *Journal of Hydrology, 492*, 89–101. https://doi.org/10.1016/j.jhydrol.2013.04.001
69. Ajmal, M., Waseem, M., Ahn, J.-H., & Kim, T.-W. (2015). Improved runoff estimation using event-based rainfall-runoff models. *Water Resources Management, 29*(6), 1995–2010. https://doi.org/10.1007/s11269-015-0924-z
70. Gupta, H. V., Sorooshian, S., & Yapo, P. O. (1999). Status of automatic calibration for hydrologic models: Comparison with multilevel expert calibration. *Journal of Hydrologic Engineering*, *4*(2). https://doi.org/10.1061/(asce)1084-0699(1999)4:2(135)